Tune-Out and Magic Wavelengths for Ground-State $^{23}Na^{40}K$ Molecules

Roman Bause,[1,2,*] Ming Li,[3] Andreas Schindewolf,[1,2] Xing-Yan Chen,[1,2] Marcel Duda,[1,2] Svetlana Kotochigova,[3] Immanuel Bloch,[1,2,4] and Xin-Yu Luo[1,2]

[1]*Max-Planck-Institut für Quantenoptik, Garching 85748, Germany*
[2]*Munich Center for Quantum Science and Technology, München 80799, Germany*
[3]*Department of Physics, Temple University, Philadelphia, Pennsylvania 19122, USA*
[4]*Fakultät für Physik, Ludwig-Maximilians-Universität, München 80799, Germany*

(Received 21 December 2019; accepted 15 June 2020; published 6 July 2020)

We demonstrate a versatile, state-dependent trapping scheme for the ground and first excited rotational states of $^{23}Na^{40}K$ molecules. Close to the rotational manifold of a narrow electronic transition, we determine tune-out frequencies where the polarizability of one state vanishes while the other remains finite, and a magic frequency where both states experience equal polarizability. The proximity of these frequencies of only 10 GHz allows for dynamic switching between different trap configurations in a single experiment, while still maintaining sufficiently low scattering rates.

DOI: 10.1103/PhysRevLett.125.023201

Trapping potentials for ultracold atoms and molecules are based on spatially dependent energy shifts of their internal states produced by magnetic, electric, or optical fields. Generally, these energy shifts are state dependent, which greatly affects the time evolution of superposition states of atoms or molecules. Demand in precision quantum metrology, simulation and computation have motivated the careful design of state-dependent traps that offer better control over quantum states. One limiting case is the magic trapping condition, where the light shift of two internal states is identical [1–3]. It is a key ingredient for achieving long coherence time in atomic and molecular clocks [4–6]. Another limiting case is the tune-out condition, where the light shift of one state vanishes while the other remains finite [7,8]. Such highly state-dependent potentials can be used in novel cooling schemes for atoms [9], selective addressing and manipulation of quantum states [10–12]. Tune-out wavelengths have also been used for precision measurements of atomic structure [13–18].

We extend these concepts to rotational states of ultracold polar molecules [19–28]. Such molecules offer unique possibilities for quantum engineering due to their strong long-range dipolar interactions and long single-particle lifetime [29–33]. Manipulating their rotational degrees of freedom is particularly important for experimental control of dipolar interactions. Though significant advances in controlling the internal states of molecules have been made [34–40], engineering rotational states in optical dipole traps remains technically challenging. This is due to both the complex level structure of molecules and the strong anisotropic coupling between the rotation of molecules and optical trapping fields. In far-detuned optical dipole traps, rotational magic conditions only exist at special light polarizations or intensities [3,41–44]. This results in a high sensitivity to polarization or intensity fluctuations, which limits rotational coherence times. Additionally, tune-out conditions, which could be powerful tools for evaporative cooling in optical lattices, have never been demonstrated for polar molecules. In this work, we demonstrate a versatile, rotational-state dependent trapping scheme by using laser light near-resonant with rotational transition lines of a nominally forbidden molecular transition. This allows us to create tune-out and magic conditions for rotational states of molecules by controlling the laser frequency, with first- and second-order insensitivity to the polarization angle and intensity of light.

In our experiments, we use $^{23}Na^{40}K$ molecules in their rovibrational ground state $|X^1\Sigma^+, v = 0, J = 0\rangle$ as well as their first rotationally excited state, $|J = 1, m_J = 0\rangle$. In the following, we will refer to these states as $|0\rangle$ and $|1\rangle$, respectively. The rotational-state dependent dipole trap is realized with laser light slightly detuned from the $|X^1\Sigma^+, v = 0, J = 0\rangle \leftrightarrow |b^3\Pi_0, v' = 0, J' = 1\rangle$ transition (subsequently called the $X \leftrightarrow b$ transition), which was previously studied in [45,46]. For detunings from this transition comparable to the rotational constants, dynamic polarizabilities depend strongly on the rotational level of the X state (see Fig. 1). Tune-out conditions for both states as well as a magic condition can thereby be achieved within

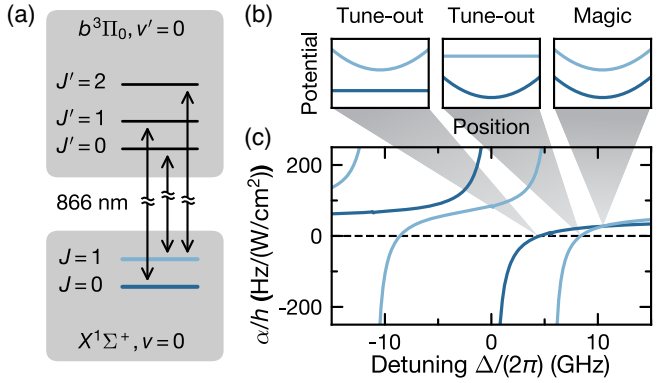

FIG. 1. Overview of the rotational-state dependent trapping scheme near the $X \leftrightarrow b$ transition. (a) Level diagram of the NaK molecule containing the $X \leftrightarrow b$ transition and the two nearest transitions from $|1\rangle$. (b) Schematic depiction of the potential experienced by $|0\rangle$ (dark blue) and $|1\rangle$ (bright blue) molecules in a dipole trap at the tune-out detuning for $|0\rangle$ (left panel), a tune-out detuning for $|1\rangle$ (center panel) and the magic detuning (right panel). (c) Frequency-dependent polarizability for $|0\rangle$ (dark blue) and $|1\rangle$ (bright blue), assuming light polarization parallel to the quantization axis. Each pole corresponds to one of the transitions shown in (a).

a frequency range of less than 10 GHz. All intermediate ratios of polarizability can be realized between these limiting cases. The $X \leftrightarrow b$ transition is mostly electric-dipole forbidden and therefore exhibits a narrow partial linewidth of $\Gamma = 2\pi \times 301(10)$ Hz, which is a measure of the decay rate from an initial state to a specific final state. This value is much smaller than the spacing between rotational states, which leads to photon scattering rates small enough to realize dipole traps at the tune-out and magic frequencies.

The frequency of the $X \leftrightarrow b$ transition is $\omega_0 = 2\pi \times 346.12358(7)$ THz, corresponding to a wavelength of $\lambda = 866.1428(3)$ nm. The polarizabilities $\alpha_0(\Delta)$ and $\alpha_1(\Delta)$ of a molecule in $|0\rangle$ or $|1\rangle$, respectively, in a light field detuned by Δ from the $X \leftrightarrow b$ transition can be described by

$$\alpha_0 = -\frac{3\pi c^2}{2\omega_0^3}\frac{\Gamma}{\Delta} + \alpha_{\mathrm{iso}}, \tag{1}$$

$$\alpha_1 = -\frac{3\pi c^2}{2\omega_0^3}\left(\frac{\Gamma\cos^2\theta}{\Delta + 2(B+B')/\hbar} + \frac{1}{5}\frac{\Gamma(\cos^2\theta + 3)}{\Delta - 2(2B' - B)/\hbar}\right) + \alpha_{\mathrm{iso}} + \alpha_{\mathrm{ang}}(\theta) \tag{2}$$

in the case where Δ is much larger than the hyperfine structure of the resonance. Here, α_{iso} and $\alpha_{\mathrm{ang}}(\theta)$ are background terms that describe the polarization-independent and -dependent contributions from the other far-detuned transitions, respectively, θ denotes the angle between the light polarization and the quantization axis, which is given by the direction of the dc electric field in the experiment. B and B' denote the ground and excited-state rotational constants, respectively. The background polarizability terms can be expressed as [2,42,47]

$$\alpha_{\mathrm{iso}} = \frac{1}{3}(\alpha_{\mathrm{bg}}^{\parallel} + 2\alpha_{\mathrm{bg}}^{\perp}), \tag{3}$$

$$\alpha_{\mathrm{ang}} = \frac{2}{15}[3\cos^2(\theta) - 1](\alpha_{\mathrm{bg}}^{\parallel} - \alpha_{\mathrm{bg}}^{\perp}), \tag{4}$$

where $\alpha_{\mathrm{bg}}^{\parallel}$ and $\alpha_{\mathrm{bg}}^{\perp}$ are the background parallel and perpendicular polarizabilities, respectively. The photon scattering rate of molecules in $|0\rangle$ near the $X \leftrightarrow b$ transition is given by

$$\gamma_{\mathrm{sc}} = \frac{3\pi c^2}{2\hbar\omega_0^3}\frac{\Gamma\Gamma_e}{\Delta^2} I, \tag{5}$$

where I is the light intensity and Γ_e is the natural linewidth of the excited state.

Our experimental cycle begins with the preparation of a near-degenerate sample of molecules in the $|0\rangle$ state using STIRAP, as described in [48]. Depending on the measurement, this preparation is done either in a far-detuned crossed-beam optical dipole trap or a one- or three-dimensional (1D or 3D) optical lattice, see the Supplemental Material [49]. All our measurements are performed at a magnetic field of 85.4 G. The $1/e$ radius of the molecule cloud is ≈ 30 μm. In order to image the molecules, we perform a reverse STIRAP procedure and employ absorption imaging on molecules in the resulting Feshbach-molecule state $|\mathrm{FB}\rangle$. To measure the effect of light at small detuning from the $X \leftrightarrow b$ transition on the molecules, we illuminate them with a laser beam at a given detuning Δ. This beam is subsequently called the 866-nm beam and is provided by a Ti:sapphire laser locked to a wavelength meter with a systematic frequency error of less than 50 MHz [57]. This is considered in all frequency errors given in the following. The 866-nm beam is focused to a spot of $1/e^2$-radius 75 μm, such that molecules experience an average intensity I of up to 2700 W/cm^2.

To directly measure the frequency-dependent polarizability $\alpha_0(\Delta)$ of molecules in the state $|0\rangle$, we prepared molecules in the crossed dipole trap. The 866-nm beam was turned on during one of the STIRAP pulses and the resulting shift of the STIRAP two-photon resonance was used to determine α_0 [49]. As shown in Fig. 2(a), the data for α_0 agree well with the theory curve given by Eq. (1) with parameters determined from the intensity-independent measurements described later.

The tune-out detuning for the $|0\rangle$ state was also measured with molecules in the crossed dipole trap. In addition to the trap, the 866-nm beam was turned on and modulated for 160 ms with 100% peak-to-peak amplitude at a frequency of 110 Hz, equal to the strongest heating resonance of the dipole trap. After this procedure, we measured the molecule cloud size by determining the root-mean-squared deviation

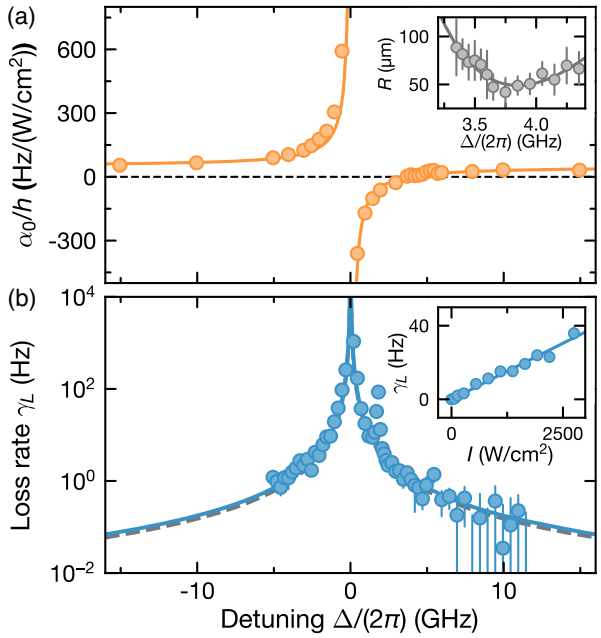

FIG. 2. Polarizability and loss rate of molecules in state $|0\rangle$. (a) Experimental data for polarizability $\alpha_0(\Delta)$ (orange circles) and theoretical curve determined using parameters from intensity-independent measurements (orange line.) The black dashed line indicates zero. Inset: Determination of the tune-out detuning for $|0\rangle$ by measuring cloud size after resonant heating. Grey circles are root-mean-square cloud sizes and the solid line is a fit used to find the minimum, see [49]. (b) Observed loss rate γ_L of molecules in $|0\rangle$ subjected to 866-nm light at an intensity of 1150 W/cm^2 (blue circles). The loss rate at $I = 0$ was subtracted from these data points. The blue solid line is a fit of Eq. (5) with ω_0 and Γ_e as the fit parameters, where data points between $\Delta = 2\pi \times 1.5$ GHz and $\Delta = 2\pi \times 2.5$ GHz were excluded to avoid biasing the fit. The grey dashed line shows the prediction of the photon scattering rate γ_{sc} assuming $\Gamma_e = 2\pi \times 11.1$ kHz. Error bars denote the standard error of the fit. Inset: Intensity dependence of the loss rate at $\Delta = 2\pi \times 1$ GHz. The solid line is a linear fit to the data.

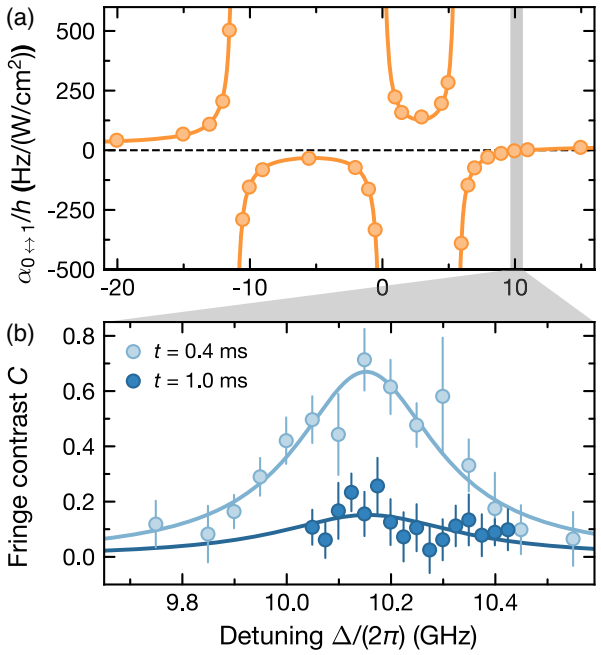

FIG. 3. Differential polarizability and magic detuning. (a) Experimental data for differential polarizability $\alpha_{0\leftrightarrow1}$ from microwave spectroscopy (orange circles) and fit to the data (orange line). The fit function is a combination of three resonances as described by Eq. (1), with a constant offset as well as the linewidths and positions for each resonance as fit parameters. (b) Determination of the magic detuning Δ_m via Ramsey spectroscopy. Bright (dark) blue circles are experimentally measured contrast after free evolution time $t = 0.4$ ms(1.0 ms) in the presence of 866-nm light. Lines are Lorentzian fits to the respective data sets, used to determine the center. Error bars denote one standard deviation and are determined from the covariance matrix of the fits.

of the density distribution, R, after 0.6 ms time of flight. At $\alpha_0(\Delta) = 0$, the heating effect is minimized, so that the smallest cloud size should be observed. With the data shown in the inset of Fig. 2(a), the tune-out point was determined to be located at $\Delta_0^{|0\rangle} = 2\pi \times 3.85(8)$ GHz.

In order to trap molecules in an optical dipole trap with long lifetime, the photon scattering rate must be low. We measured the radiative lifetime by illuminating molecules in state $|0\rangle$ with 866-nm light. The molecules were frozen in a far-detuned 3D optical lattice to avoid collisional loss. The molecule loss rate γ_L caused by the 866-nm beam was determined by fitting an exponential decay curve to the measured molecule numbers, see Fig. 2(b). From these data, we determined the position of the resonance feature at $\omega_0 = 2\pi \times 346.12358(7)$ THz. To ensure that this resonance was not shifted by the presence of far off-resonant dipole trap light, we performed additional loss measurements for small values of Δ with all far-detuned trapping light turned off and found a shift in resonance frequency of less than 20 MHz. A calculation with the optical potential method shows that molecules in the $|b^3\Pi_0\rangle$ state predominantly decay into states in the $|a^3\Sigma^+\rangle$ manifold [49]. We can therefore assume that every photon scattering event leads to the loss of a molecule, such that $\gamma_L \approx \gamma_{sc}$. Under this assumption, our experimental data yields a value of $\Gamma_e = 13.0(5)$ kHz, which is in agreement with the theoretical value of $\Gamma_e = 11.1$ kHz. We additionally investigated the dependence of γ_L on the light intensity, see inset of Fig. 2(b). The observed linear dependence excludes the presence of two-photon scattering processes in this frequency range. At $\Delta = 2\pi \times 1.78(5)$ GHz we observed a second, smaller loss peak, which we hypothesize could be a transition to a state in the $|b^3\Pi_{0^-}\rangle$ manifold [49]. Still, at all detunings relevant for rotational-state dependent trapping, we find loss rates low enough that lifetimes of more than 1 s can be achieved in a 866-nm trap with a depth of $k_B \times 1$ μK.

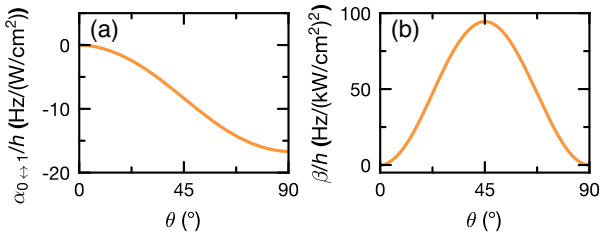

FIG. 4. Dependence of (a) differential polarizability $\alpha_{0\leftrightarrow1}$ and (b) hyperpolarizability β in $|1\rangle$ on light polarization angle θ at the magic detuning with a dc electric field of 86 V/cm. β represents the second-order dependence of the light shift on the light intensity [49].

To determine quantities associated with the excited rotational state $|1\rangle$, we trapped molecules in a spin-decoupled 1D magic lattice described in [42]. To decouple rotation from nuclear spin and trapping light field, and allow for a well-defined transition to $|1\rangle$, we employed a dc electric field of 86 V/cm such that the angle between the polarization of the 866-nm light and the electric field was 4 (2)°. The differential polarizability $\alpha_{0\leftrightarrow1} = \alpha_1 - \alpha_0$ was measured via microwave spectroscopy [49]. The resulting data agree with Eqs. (1) and (2), see Fig. 3(a).

The magic detuning can be accurately measured via Ramsey spectroscopy of the $|0\rangle \leftrightarrow |1\rangle$ transition, which consists of two resonant $\pi/2$ microwave pulses separated by a free evolution period with duration t. We varied the phase ϕ of the second microwave pulse for a given t to obtain Ramsey fringes. During the free evolution period, the 866-nm beam was turned on. Any inhomogeneous broadening of the microwave resonance due to the differential light shift of the 866-nm light reduces the contrast of $N_0(\phi)$. Therefore, the magic detuning is identified as the maximum of fringe contrast. By fitting a Lorentzian to the contrast data, see Fig. 3(b), we determined the magic detuning to be $\Delta_m = 2\pi \times 10.15(6)$ GHz. The shift of Δ_m due to the 4° misalignment of θ is negligible compared to other error sources. Both the first- and second-order differential light shifts vanish and are first-order insensitive to polarization imperfections at $\theta = 0°$ as shown in Fig. 4. Thus, if $|\theta| \leq 0.5°$, the differential light shift of the 866-nm light at magic detuning can be a factor of 70 smaller than that of a typical magic polarization trap. In the present experiments, the coherence time is limited to about 1 ms mostly by inhomogeneities of the electric field. Our simulation shows that a coherence time of 30 ms in a 866-nm magic trap is feasible if the electric field fluctuation is less than 0.3 mV/cm [49]. Alternatively, the electric field could be replaced by a strong magnetic field for decoupling the rotation and nuclear spins by Zeeman splitting. The weak coupling between the rotation and magnetic field could allow for longer coherence times.

We can uniquely determine the shape of the polarizability curve $\alpha_0(\Delta)$ from two frequencies that were measured in an intensity-independent manner. The first of these is the tune-out detuning $\Delta_0^{|0\rangle}$. The second is the point where the two-photon detuning of STIRAP between the Feshbach-molecule state $|\mathrm{FB}\rangle$ and the state $|0\rangle$ becomes insensitive to the 866-nm light intensity. This is achieved at a detuning $\Delta^\star$ where molecules in $|\mathrm{FB}\rangle$ and $|0\rangle$ experience the same light shift [49,58]. From these two measured detunings and the value of ω_0, we computed the partial linewidth of the $X \leftrightarrow b$ transition Γ as well as the isotropic background polarizability α_{iso} via Eq. (1). The location of the poles of Eq. (2) and the known ground-state rotational constant B were used to determine the excited-state rotational constant B'. To find the values of the background polarizability terms $\alpha_{\mathrm{bg}}^{\parallel}$ and $\alpha_{\mathrm{bg}}^{\perp}$, we used the known form of $\alpha_0(\Delta)$ as well as Eqs. (3)–(4) and required the differential polarizability $\alpha_{0\leftrightarrow1}$ to be zero at the measured value of Δ_m. Finally, using Γ and the background polarizability terms, we determined the two tune-out detunings of the state $|1\rangle$ to the left and the right of the $J = 1 \leftrightarrow J' = 2$ transition, $\Delta_0^{|1\rangle,l}$ and $\Delta_0^{|1\rangle,r}$. In combination, these quantities, summarized in Table I, fully describe the behavior of molecules in the presence of light near the $X \leftrightarrow b$ transition.

TABLE I. Summary of the molecular response at the $X \leftrightarrow b$ transition. Our values of ω_0 and B' are compared to literature values for the ^{23}Na^{39}K molecule.

Quantity	Value	Reference
ω_0	$2\pi \times 346.12358(7)$ THz	This work
	$2\pi \times 346.1434$ THz	[46] (for ^{23}Na^{39}K)
Γ	$2\pi \times 301(10)$ Hz	This work
Γ_e	$2\pi \times 13.0(5)$ kHz	This work
$\alpha_{\mathrm{bg}}^{\parallel}$	$h \times 105(3)$ Hz/(W/cm^2)	This work
$\alpha_{\mathrm{bg}}^{\perp}$	$h \times 20(1)$ Hz/(W/cm^2)	This work
B'	$h \times 2.79(2)$ GHz	This work
	$h \times 2.85$ GHz	[46] (for ^{23}Na^{39}K)
B	$h \times 2.8217297(10)$ GHz	[37]
$\Delta_0^{\|0\rangle}$	$2\pi \times 3.85(8)$ GHz	This work
$\Delta_0^{\|1\rangle,l}$	$-2\pi \times 8.93(15)$ GHz	This work
$\Delta_0^{\|1\rangle,r}$	$2\pi \times 7.95(15)$ GHz	This work
Δ_m	$2\pi \times 10.15(6)$ GHz	This work
$\Delta^\star$	$-2\pi \times 6.78(17)$ GHz	This work

In conclusion, we have demonstrated a versatile rotational-state dependent optical dipole trap by utilizing a nominally forbidden electronic transition from the singlet ground state to the lowest electronically excited triplet state of ^{23}Na^{40}K molecules. We precisely determined a tune-out frequency for the ground-state molecules by resonant modulation heating spectroscopy and a magic frequency of rotational states by Ramsey interferometry. Our results open new ways to address key challenges in the field of ultracold polar molecules: for example, trapping molecules in a lattice at one of the tune-out wavelengths would allow

selective transfer of hotter molecules at the edge of the lattice into the nontrapped state, thus removing entropy from the sample. In such a lattice, the molecules could thermalize via long-range interactions and would be protected from collisional loss by Pauli blocking [59] or dipole blocking [60], thereby enabling evaporative cooling. The close proximity of the tune-out and magic frequencies allows dynamic switching or even continuous modulation between trap configurations with arbitrary ratios of polarizability experienced by different rotational states. This may open up new possibilities for Floquet engineering of topological states in dipolar spin systems [61] or other novel methods of dynamic control of quantum systems. Another natural application of light near-resonant to the $X \leftrightarrow b$ transition is to create repulsive potentials for ultracold molecules, e.g., to trap them in the dark. Due to the low photon scattering rates at small positive detuning, one can generate a repulsive box trap with sufficiently low intensity in its center to allow investigation of the proposed photon-assisted loss of scattering complexes of molecules [62–64]. Our methods can be generalized to other species of ultracold bialkali molecules by carefully choosing a similar narrow molecular transition.

We thank Y. Bao, H. Bekker, A. Christianen, O. Dulieu, J. He, T. Shi, D. Wang, and T. Zelevinsky for stimulating discussions. We thank C. Gohle, F. Seeßelberg, and S. Eustice for their contributions to the experiment. The MPQ team gratefully acknowledges support from the Max Planck Society, the European Union (PASQuanS Grant No. 817482) and the Deutsche Forschungsgemeinschaft under Germany's Excellence Strategy EXC-2111 390814868 and under Grant No. FOR 2247. Work at Temple University is supported by the Army Research Office Grant No. W911NF-17-1-0563, the U.S. Air Force Office of Scientific Research Grant No. FA9550-14-1-0321 and the NSF Grant No. PHY-1908634.

*roman.bause@mpq.mpg.de

[1] H. Katori, T. Ido, and M. Kuwata-Gonokami, J. Phys. Soc. Jpn. **68**, 2479 (1999).
[2] S. Kotochigova and D. DeMille, Phys. Rev. A **82**, 063421 (2010).
[3] B. Neyenhuis, B. Yan, S. A. Moses, J. P. Covey, A. Chotia, A. Petrov, S. Kotochigova, J. Ye, and D. S. Jin, Phys. Rev. Lett. **109**, 230403 (2012).
[4] J. Ye, H. J. Kimble, and H. Katori, Science **320**, 1734 (2008).
[5] S. S. Kondov, C.-H. Lee, K. H. Leung, C. Liedl, I. Majewska, R. Moszynski, and T. Zelevinsky, Nat. Phys. **15**, 1118 (2019).
[6] K. H. Leung, I. Majewska, H. Bekker, C.-H. Lee, E. Tiberi, S. S. Kondov, R. Moszynski, and T. Zelevinsky, arXiv:2005.12400.
[7] L. J. LeBlanc and J. H. Thywissen, Phys. Rev. A **75**, 053612 (2007).
[8] B. Arora, M. S. Safronova, and C. W. Clark, Phys. Rev. A **84**, 043401 (2011).
[9] J. Catani, G. Barontini, G. Lamporesi, F. Rabatti, G. Thalhammer, F. Minardi, S. Stringari, and M. Inguscio, Phys. Rev. Lett. **103**, 140401 (2009).
[10] S. Kotochigova and E. Tiesinga, Phys. Rev. A **73**, 041405 (R) (2006).
[11] Y. Wang, X. Zhang, T. A. Corcovilos, A. Kumar, and D. S. Weiss, Phys. Rev. Lett. **115**, 043003 (2015).
[12] A. Rubio-Abadal, J.-Y. Choi, J. Zeiher, S. Hollerith, J. Rui, I. Bloch, and C. Gross, Phys. Rev. X **9**, 041014 (2019).
[13] W. F. Holmgren, R. Trubko, I. Hromada, and A. D. Cronin, Phys. Rev. Lett. **109**, 243004 (2012).
[14] C. D. Herold, V. D. Vaidya, X. Li, S. L. Rolston, J. V. Porto, and M. S. Safronova, Phys. Rev. Lett. **109**, 243003 (2012).
[15] A. Petrov, C. Makrides, and S. Kotochigova, Mol. Phys. **111**, 1731 (2013).
[16] B. M. Henson, R. I. Khakimov, R. G. Dall, K. G. H. Baldwin, L.-Y. Tang, and A. G. Truscott, Phys. Rev. Lett. **115**, 043004 (2015).
[17] W. Kao, Y. Tang, N. Q. Burdick, and B. L. Lev, Opt. Express **25**, 3411 (2017).
[18] A. Heinz, A. J. Park, J. Trautmann, N. Šantić, S. G. Porsev, M. S. Safronova, I. Bloch, and S. Blatt, Phys. Rev. Lett. **124**, 203201 (2020).
[19] K.-K. Ni, S. Ospelkaus, M. H. G. de Miranda, A. Peer, B. Neyenhuis, J. J. Zirbel, S. Kotochigova, P. S. Julienne, D. S. Jin, and J. Ye, Science **322**, 231 (2008).
[20] T. Takekoshi, L. Reichsöllner, A. Schindewolf, J. M. Hutson, C. R. LeSueur, O. Dulieu, F. Ferlaino, R. Grimm, and H.-C. Nägerl, Phys. Rev. Lett. **113**, 205301 (2014).
[21] P. K. Molony, P. D. Gregory, Z. Ji, B. Lu, M. P. Köppinger, C. R. LeSueur, C. L. Blackley, J. M. Hutson, and S. L. Cornish, Phys. Rev. Lett. **113**, 255301 (2014).
[22] J. W. Park, S. A. Will, and M. W. Zwierlein, Phys. Rev. Lett. **114**, 205302 (2015).
[23] M. Guo, B. Zhu, B. Lu, X. Ye, F. Wang, R. Vexiau, N. Bouloufa-Maafa, G. Quéméner, O. Dulieu, and D. Wang, Phys. Rev. Lett. **116**, 205303 (2016).
[24] D. J. McCarron, M. H. Steinecker, Y. Zhu, and D. DeMille, Phys. Rev. Lett. **121**, 013202 (2018).
[25] T. M. Rvachov, H. Son, A. T. Sommer, S. Ebadi, J. J. Park, M. W. Zwierlein, W. Ketterle, and A. O. Jamison, Phys. Rev. Lett. **119**, 143001 (2017).
[26] H. Yang, D.-C. Zhang, L. Liu, Y.-X. Liu, J. Nan, B. Zhao, and J.-W. Pan, Science **363**, 261 (2019).
[27] L. R. Liu, J. D. Hood, Y. Yu, J. T. Zhang, K. Wang, Y.-W. Lin, T. Rosenband, and K.-K. Ni, Phys. Rev. X **9**, 021039 (2019).
[28] L. Anderegg, L. W. Cheuk, Y. Bao, S. Burchesky, W. Ketterle, K.-K. Ni, and J. M. Doyle, Science **365**, 1156 (2019).
[29] L. D. Carr, D. DeMille, R. V. Krems, and J. Ye, New J. Phys. **11**, 055049 (2009).
[30] M. A. Baranov, M. Dalmonte, G. Pupillo, and P. Zoller, Chem. Rev. **112**, 5012 (2012).
[31] M. P. Kwasigroch and N. R. Cooper, Phys. Rev. A **96**, 053610 (2017).
[32] J. L. Bohn, A. M. Rey, and J. Ye, Science **357**, 1002 (2017).

[33] K.-K. Ni, T. Rosenband, and D. D. Grimes, Chem. Sci. **9**, 6830 (2018).
[34] S. Ospelkaus, K.-K. Ni, G. Quéméner, B. Neyenhuis, D. Wang, M. H. G. de Miranda, J. L. Bohn, J. Ye, and D. S. Jin, Phys. Rev. Lett. **104**, 030402 (2010).
[35] B. Yan, S. A. Moses, B. Gadway, J. P. Covey, K. R. A. Hazzard, A. M. Rey, D. S. Jin, and J. Ye, Nature (London) **501**, 521 (2013).
[36] P. D. Gregory, J. Aldegunde, J. M. Hutson, and S. L. Cornish, Phys. Rev. A **94**, 041403(R) (2016).
[37] S. A. Will, J. W. Park, Z. Z. Yan, H. Loh, and M. W. Zwierlein, Phys. Rev. Lett. **116**, 225306 (2016).
[38] A. Prehn, M. Ibrügger, R. Glöckner, G. Rempe, and M. Zeppenfeld, Phys. Rev. Lett. **116**, 063005 (2016).
[39] M. Guo, X. Ye, J. He, G. Quéméner, and D. Wang, Phys. Rev. A **97**, 020501(R) (2018).
[40] L. Caldwell, H. J. Williams, N. J. Fitch, J. Aldegunde, J. M. Hutson, B. E. Sauer, and M. R. Tarbutt, Phys. Rev. Lett. **124**, 063001 (2020).
[41] P. D. Gregory, J. A. Blackmore, J. Aldegunde, J. M. Hutson, and S. L. Cornish, Phys. Rev. A **96**, 021402(R) (2017).
[42] F. Seeßelberg, X.-Y. Luo, M. Li, R. Bause, S. Kotochigova, I. Bloch, and C. Gohle, Phys. Rev. Lett. **121**, 253401 (2018).
[43] J. A. Blackmore, L. Caldwell, P. D. Gregory, E. M. Bridge, R. Sawant, J. Aldegunde, J. Mur-Petit, D. Jaksch, J. M. Hutson, B. E. Sauer, M. R. Tarbutt, and S. L. Cornish, Quantum Sci. Technol. **4**, 014010 (2018).
[44] T. Rosenband, D. D. Grimes, and K.-K. Ni, Opt. Express **26**, 19821 (2018).
[45] J. Kobayashi, K. Aikawa, K. Oasa, and S. Inouye, Phys. Rev. A **89**, 021401(R) (2014).
[46] H. Harker, P. Crozet, A. J. Ross, K. Richter, J. Jones, C. Faust, J. Huennekens, A. V. Stolyarov, H. Salami, and T. Bergeman, Phys. Rev. A **92**, 012506 (2015).
[47] M. Li, A. Petrov, C. Makrides, E. Tiesinga, and S. Kotochigova, Phys. Rev. A **95**, 063422 (2017).
[48] F. Seeßelberg, N. Buchheim, Z.-K. Lu, T. Schneider, X.-Y. Luo, E. Tiemann, I. Bloch, and C. Gohle, Phys. Rev. A **97**, 013405 (2018).
[49] See the Supplemental Material at http://link.aps.org/supplemental/10.1103/PhysRevLett.125.023201 for the theory of molecule polarizability, details on the experimental setup, fit functions for tune-out and magic frequencies, intensity calibration, example data for polarizability, theoretical computation of linewidths, lifetime measurements, and polarization dependence of polarizability, which includes Refs. [50–56].
[50] R. V. Krems, *Molecules in Electromagnetic Fields: From Ultracold Physics to Controlled Chemistry* (John Wiley & Sons, Hoboken, 2018).
[51] M. E. Gehm, K. M. O'Hara, T. A. Savard, and J. E. Thomas, Phys. Rev. A **58**, 3914 (1998).
[52] R. Grimm, M. Weidemüller, and Y. B. Ovchinnikov, in *Advances in Atomic, Molecular, and Optical Physics* (Elsevier, Cambridge, 2000), pp. 95–170.
[53] M. Safronova, B. Arora, and C. Clark, Phys. Rev. A **73**, 022505 (2006).
[54] B. Zygelman and A. Dalgarno, Phys. Rev. A **38**, 1877 (1988).
[55] A. Gerdes, M. Hobein, H. Knöckel, and E. Tiemann, Eur. Phys. J. D **49**, 67 (2008).
[56] M. Aymar and O. Dulieu, Mol. Phys. **105**, 1733 (2007).
[57] L. Couturier, I. Nosske, F. Hu, C. Tan, C. Qiao, Y. H. Jiang, P. Chen, and M. Weidemüller, Rev. Sci. Instrum. **89**, 043103 (2018).
[58] R. Vexiau, D. Borsalino, M. Lepers, A. Orbán, M. Aymar, O. Dulieu, and N. Bouloufa-Maafa, Int. Rev. Phys. Chem. **36**, 709 (2017).
[59] A. Chotia, B. Neyenhuis, S. A. Moses, B. Yan, J. P. Covey, M. Foss-Feig, A. M. Rey, D. S. Jin, and J. Ye, Phys. Rev. Lett. **108**, 080405 (2012).
[60] A. Micheli, G. Pupillo, H. P. Büchler, and P. Zoller, Phys. Rev. A **76**, 043604 (2007).
[61] T. Schuster, F. Flicker, M. Li, S. Kotochigova, J. E. Moore, J. Ye, and N. Y. Yao, arXiv:1901.08597.
[62] A. Christianen, M. W. Zwierlein, G. C. Groenenboom, and T. Karman, Phys. Rev. Lett. **123**, 123402 (2019).
[63] P. D. Gregory, J. A. Blackmore, S. S. Bromley, and S. L. Cornish, Phys. Rev. Lett. **124**, 163402 (2020).
[64] Y. Liu, M.-G. Hu, M. A. Nichols, D. D. Grimes, T. Karman, H. Guo, and K.-K. Ni, arXiv:2002.05140.